

An Immersed Boundary Method for Simulation of Moving Object in Fluid Flow

Pham Van Sang

Hanoi University of Science and Technology, No. 1, Dai Co Viet, Hai Ba Trung, Hanoi, Viet Nam

Received: November 29, 2017; Accepted: May 25, 2018

Abstract

Numerical modelling for the interaction between fluid flow interacting and moving object is a quite complicated problem in computational engineering. Such modelling requires solving simultaneously Navier-Stokes equation for fluid flow and Newton equation for object motion. Due to the motion, computational mesh needs to be re-generated in every time step, making the modelling complicated and time consuming. In this paper, we introduce a numerical method which utilizes immersed boundary to represent motion of solid object under effect of 3-dimension fluid flow. In the current method, we developed a numerical method for enforcing viscous boundary conditions on the immersed boundary. The method was validated and applied to simulate the inertial focusing of solid particle in spiral channel, obtained result well matches with experimental observation indicating the accuracy of the developed method.

Keywords: Immersed boundary method, Newton equations, Inertial sorting, Dean flow

1. Introduction

In computational fluid dynamics, simulations of fluid-structure interaction problems are normally obstructed by complexity of computational domain and the motion of the structure which leads to the change of the computational mesh during solving process. Finite volume and finite element methods have been shown to be usable approaches for simulating such problems. However, these methods are computationally expensive for moving object simulation where the unstructured mesh requires regeneration in each time step. In 3D, parallel simulation, process of mesh regeneration takes a long time to generate new mesh, redistribute the mesh over the processes community, and re-calculate the discretization matrix...

An alternative method recently employed in simulation of fluid-structure interaction is the immersed boundary method (IBM). In this method, the presence of structure in flow field is represented by an additional forcing term in the equations for fluid flow rather than a body-fitted mesh. Therefore, flow over a complex geometry can be easily handled with orthogonal, structured mesh. The advantages of the IBM are reducing computation time, and easy mesh generation.

In this study, we present an immersed boundary method for fluid-structure interaction. Boundary conditions for fluid flow and structure are satisfied by

a set of procedures which enforcing the conditions at the spatial location of structure-fluid boundary. The method was validated and applied to simulate the inertial focusing of solid particle in spiral channel, obtained result well matches with experimental observation indicating the accuracy of the developed method and showing feasible ability of applying the method in developing a numerical solver for predicting and optimizing design of microfluidics sorting devices using in medicine.

In the following sections, we first present the numerical method for solving the coupling of fluid flow and object motion. A validation for the method is then provided, and we apply the method in simulation an actual microfluidics inertial sorting and separating problems.

2. Numerical method

We consider problem model of an object moving freely in fluid flow as sketched in Fig. 1. Having assumption that the object is solid; the fluid flow and object motion are governed by Navier-Stokes equations and Newton equations, respectively:

$$\frac{\partial u_i}{\partial t} = \nu_f \frac{\partial^2 u_i}{\partial x_j^2} - \frac{\partial u_j u_i}{\partial x_j} - \frac{1}{\rho_f} \frac{\partial p}{\partial x_i} + f \quad (1)$$

$$\frac{\partial u_i}{\partial x_i} = 0 \quad (2)$$

* Corresponding author: Tel.: (+84) 966633683
Email: sang.phamvan@hust.edu.vn

$$m_p \frac{du_p}{dt} = \rho_f \oint_{\Gamma_p} \tau \cdot n ds + V_p (\rho_p - \rho_f) \mathbf{g} \quad (3)$$

$$I_p \frac{d\omega_p}{dt} = \rho_f \oint_{\Gamma_p} \mathbf{r} \cdot (\boldsymbol{\tau} \times \mathbf{n}) ds \quad (4)$$

In above equations, $\mathbf{u} = (u_x, u_y, u_z)$ is fluid velocity vector, p is static pressure, $\mathbf{u}_p = (u_{px}, u_{py}, u_{pz})$ is translational velocity of the object, $\boldsymbol{\omega}_p = (\omega_{px}, \omega_{py}, \omega_{pz})$ is angular velocity of the object, is the hydrodynamic stress tensor cause by the motion of particle in the fluid, \mathbf{n} is the normal vector outward pointing from the particle surface, \mathbf{g} is the gravitational acceleration, \mathbf{r} is the vector connecting the center of particle and a point on its surface (Γ_p).

Other parameters including ν , ρ_f , m_p , V_p , ρ_p , I_p are kinematic viscosity, volume density of the fluid, mass of the particle, volume of the particle, volume density of the particle, and moment of inertia of the particle, respectively.

In IBM, computational domain is defined by a fixed Cartesian grid. A solid object in the computational domain is represented by an immersed boundary which is defined by a number of points (which are referred as Lagrangian force points). The Cartesian grid and immersed boundary are illustrated in Fig.1. The Lagrangian points are not required to be coincident with Cartesian grid points (which are referred as Eulerian points). In term of IBM, effects of the solid object on the fluid flow are represented by the addition of a forcing term in the equation for the conservation of momentum (1).

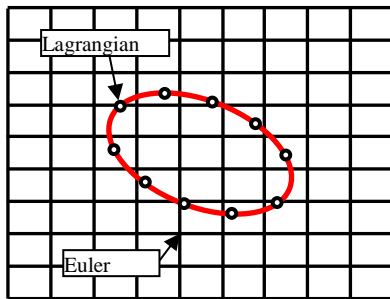


Fig.1. Fixed Eulerian for physical domain representation and Lagrangian grid for structure's surface.

The forcing term, \mathbf{f} , in the momentum equation (1), is a kind of external force exerting on the flow field to represent the mutual interaction between fluid and immersed boundary. The forcing term takes a non-zero value at grid points that are in the vicinity of the

boundary, but has no effect on the computation of grid points away from the boundary. Magnitude of the forcing term is determined in such a way that the boundary condition on the immersed boundary is satisfied. To determinethe forcing term , we rearrange (1) to yield

$$\mathbf{f} = \mathbf{u}_i - \left(\nu \nabla^2 \mathbf{u} - (\mathbf{u} \cdot \nabla) \mathbf{u} - \frac{1}{\rho_f} \nabla p \right)$$

Writing the above equation at the Lagrangian points (denoted by capital letters) gives a similar equation

$$\mathbf{F} = \mathbf{U}_i - \left(\nu \nabla^2 \mathbf{U} - (\mathbf{U} \cdot \nabla) \mathbf{U} - \frac{1}{\rho_f} \nabla P \right)$$

Make use of the Euler forward method to approximate the transient term,

$$\mathbf{F} = \frac{\mathbf{U}^{k+1} - \mathbf{U}^k}{\Delta t} - \left(\nu \nabla^2 \mathbf{U} - (\mathbf{U} \cdot \nabla) \mathbf{U} - \frac{1}{\rho_f} \nabla P \right)$$

where, the superscripts k+1 and k denote continuous time levels. By introducing a temporal velocity, which satisfies the momentum equation at Lagrangian points, we get

$$\mathbf{F} = \frac{\mathbf{U}^{k+1} - \hat{\mathbf{U}}^k}{\Delta t} - \left(\frac{\hat{\mathbf{U}}^k - \mathbf{U}^k}{\Delta t} + \nu \nabla^2 \mathbf{U} - (\mathbf{U} \cdot \nabla) \mathbf{U} - \frac{1}{\rho_f} \nabla P \right)$$

Because of the satisfaction of the momentum equation at Lagrangian points, the above equation reduces to

$$\mathbf{F} = \frac{\mathbf{U}^{k+1} - \hat{\mathbf{U}}^k}{\Delta t}$$

To enforce the boundary condition on the immersed boundary surface, the velocity \mathbf{U}^{k+1} is set to the value of boundary velocity (e.g, velocity of particle surface).

Thus, we can write, $\mathbf{F} = \frac{\mathbf{U}^{(b)} - \hat{\mathbf{U}}^k}{\Delta t}$

In the most cases, Lagrangian points are not at location of Eulerian points. Therefore, force at Eulerian points is calculated from force at Lagrangian points using discrete delta function [3]

$$\mathbf{f} = \sum_{l=1}^N \mathbf{F}(x_l) \delta_h(\mathbf{x} - \mathbf{x}_l) \Delta V_l$$

where ΔV_l is discrete volume associating with each Lagrangian point. $\delta_h(\mathbf{x} - \mathbf{x}_l)$ is the delta function.

$\delta_h(x-x_l) = \delta_h^{1D}(x-x_l)\delta_h^{1D}(y-y_l)\delta_h^{1D}(z-z_l)$ With $\delta_h^{1D}(x-x_l)$ is the regularized one-dimensional delta function.

In order to couple the Navier-Stokes and Newton equations, we solve the Navier-Stokes equations by using a fractional-step method for enforcing continuity, a three-step Runge-Kutta scheme for convective terms, and the Crank-Nicholson method for the viscous terms. The spatial derivatives are evaluated by second-order finite different schemes on a staggered grid sketched. The algorithm for solving flow equations, including the fluid-solid coupling terms, and motion equations, in a Runge-Kutta step, starts by advancing the Navier-Stokes equations without forcing term:

$$\begin{aligned} \tilde{\mathbf{u}} &= \mathbf{u}^{k-1} + \Delta t(2\alpha_k \nu \nabla^2 \mathbf{u}^{k-1} - 2\alpha_k \frac{1}{\rho_f} \nabla p^{k-1} \\ &- \gamma_k ((\mathbf{u} \cdot \nabla) \mathbf{u})^{k-1} - \zeta_k ((\mathbf{u} \cdot \nabla) \mathbf{u})^{k-2}) \end{aligned}$$

Velocity at Eulerian points is then spreaded to Lagrangian points using the delta function formulation:

$$\tilde{\mathbf{U}}_{x_l} = \sum_{k=1}^N \tilde{\mathbf{u}}_k \delta_h(x-x_k) h^3$$

Forcing term is then calculated at Lagrangian points, and spreaded back to Eulerian points:

$$\mathbf{F}_{x_l} = \frac{\mathbf{U}_{x_l}^{(b)} - \tilde{\mathbf{U}}_{x_l}}{\Delta t}; \mathbf{f}_x = \sum_{l=1}^N \mathbf{F}_{x_l} \delta_h(x-x_l) \Delta V_l$$

The Navier-Stokes equation is then resolved with the obtained forcing term at Eulerian points.

$$\nabla^2 \mathbf{u}^* - \frac{\mathbf{u}^*}{\alpha_k \nu \Delta t} = -\frac{1}{\nu \alpha_k} \left(\frac{\tilde{\mathbf{u}}}{\Delta t} + \mathbf{f}_x \right) + \nabla^2 \mathbf{u}^{k-1}$$

Equations for translational and angular motion of object is solved using forcing term at Lagrangian points:

$$\begin{aligned} \mathbf{u}_p^k &= \mathbf{u}_p^{k-1} - 2\alpha_k \Delta t \frac{\rho_p \rho_f}{m_p (\rho_p - \rho_f)} \sum_{l=1}^N \mathbf{F}_{x_l} \Delta V_l + \mathbf{g} \\ \boldsymbol{\omega}_p^k &= \boldsymbol{\omega}_p^{k-1} - 2\alpha_k \Delta t \frac{\rho_p \rho_f}{I_p (\rho_p - \rho_f)} \sum_{l=1}^N (\mathbf{X}_l - \mathbf{x}_p^k) \times \mathbf{F}_{x_l} \Delta V_l \end{aligned}$$

In the above equation, α_k, γ_k and ζ_k are the coefficient of the three-step Runge-Kutta scheme. As given in [5], $\alpha_1 = 4/15, \gamma_1 = 8/15, \zeta_1 = 0, \alpha_2 = 1/15, \gamma_2 = 5/12, \zeta_2 = -17/60, \alpha_3 = 1/6, \gamma_3 = 3/4$, and $\zeta_3 = -5/12$

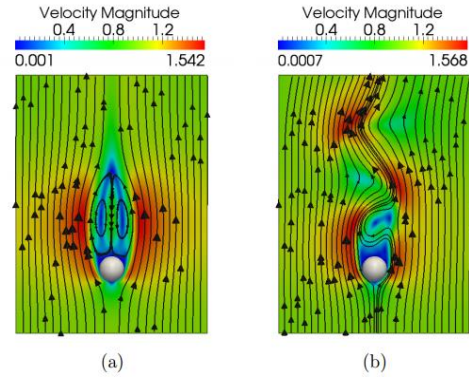


Fig 2. Flow streamlines at time step before (a) and after 5000 (b) vortex shedding forms

3. Results and discussion

3.1. Validation case

To validate the proposed method, we consider a fluid flow around a stationary circular cylinder. The cylinder is represented by an immersed boundary with by 80 Lagrangian points distributing regularly on the surface. To validate our simulation result, we compare the drag and lift forces acting on the cylinder with the published data. Flow streamlines at an early time step when the flow is still symmetry is plotted in Fig.2. As time passed, the flow becomes unstable and the symmetry breaks up, fluid flow oscillates, vortex shedding appears. Table 1 shows the drag and lift coefficients obtained with the presented numerical method and method by another author at $Re = 100$. As can be seen, our results are in a good agreement with the published results [1,2,3].

Table 1. Drag and lift coefficients of the cylinder calculated for $Re=100$.

	C_D	C_L
Braza <i>et al.</i> [2]	1.36	0.25
Liu <i>et al.</i> [3]	1.35	0.3
Calhoun <i>et al.</i> [1]	1.33	0.30
Present	1.37	0.32

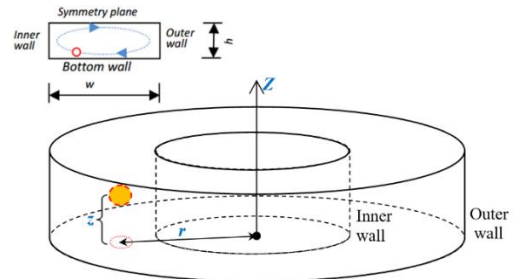


Fig. 3. Model of infinite spiral channel. Position of particle in the spiral channel is defined using a cylindrical coordinate system.

3.2. Particle in realistic Dean flow

In order to further validated the method, we are going to carry out simulation result for inertial sorting problem presented in the work published by Guan et al. (2013) [6]. In the study, Guan shown experimental results for focusing behavior of micro-size particles with various diameters in spiral channel. The results are very useful in designing device for extracting circulating tumor cell (CTC) out of blood. We conduct simulation for particle traveling in a spiral channel which is 15mm in diameter, 600 μ m in width and 120 μ m in depth. The cancer cells are modeled by spherical particles which are 15.5 μ m of diameter. The spiral channel is sketched in Fig. 3. The fluid flow volumetric rate in the channel is set at 2ml/min, this flow rate is equivalent with average velocity of 0.46m/sec of fluid flow in the channel

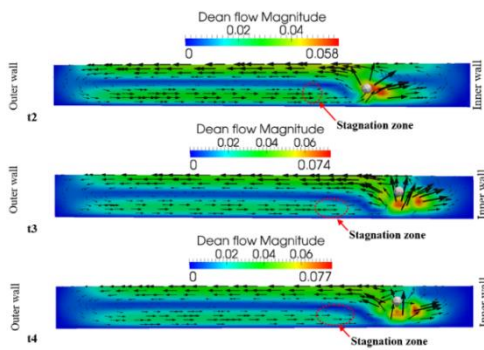


Fig. 4. Secondary flow field around particle at different time step. Secondary flow near the bottom wall push the particle towards the inner wall

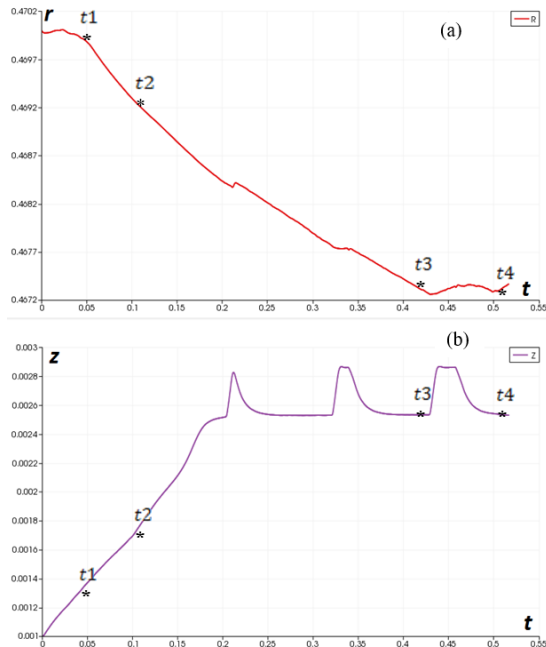


Fig. 5. Cylindrical coordinate of particle A which was located initially near the bottom wall of spiral channel.

In this problem, we concern the position of particle at steady state. Thus, we first solve for flow in the channel to obtain the steady state flow. Then, particle is located into the flow to examine its steady motion. To achieve a general result and save simulation time, particles are located at different positions: near the bottom wall where the Dean flow is coming towards the inner wall, near the symmetry plane where the Dean flow is coming towards the outer wall.

Due to the multiscale of the problem, particle size is much smaller than the channel size, the numerical model requires a fine mesh for accurate modeling results. In the current simulation, a mesh of 9.5 million elements is used. The mesh is distributed over 32 processes.

For convenience in analysis, all quantities presented in this section are dimensionless. These quantities can be converted into dimensional values using the following scales: Length scale $l_0 = 15mm$, velocity scale $v_0 = 0.46m/sec$. In dimensionless formulation, the channel diameter is 1, the channel width is 0.04, the channel height is 0.004, and the particle diameter is 0.001.

Particle focusing

In the Fig.5, position of particle is presented in cylindrical coordinates (r,z). As can be seen in Fig. 4, due to the Dean flow near the bottom wall the particle is pushed towards the inner wall. When the particle is at a distance of 0.463 from the channel centroid (or 45 μ m from the inner wall), it seems to be unable to come closer to the inner wall (as shown in Fig. 5, from $t=0.43$ to 0.52). Comparing this ‘stable state’ position of particle to the corresponding outlet position in experiment (marked by the yellow arrow Fig. 6), we can see an agreement between the experimental and numerical results.

Effect of Dean flow on particle motion

We examine effect of the Dean flow on the particle by plotting secondary velocity field around particle at different time steps (denoted by t1, t2, t3, t4 in Fig. 5). The velocity fields are shown in Fig. 4.

At early time steps (t1, t2), when particle is still far from the inner wall, it moves along the secondary flow near the bottom wall. However, the closer to the wall, the stronger wall-induce inertial lift force; the opposing forces (Dean drag force and the wall-induce force) result in a ‘stagnation zone’ (Fig. 4). The stagnation zone is expanding while the particle comes closer to the inner wall (Fig. 4). It should be noted that this ‘stagnation zone’ is defined with respect to the secondary flow (flow in channel lateral direction), the

zone of course is still flowing with the main flow in the longitudinal channel direction.

When the particle moves to a critical position, where the Dean drag and wall-induced inertial lift forces seem to be balanced, the particle is not able to come closer to the inner wall. The fluid volume surrounding the particle seems to be confined (by the Dean flow), the fluid flow inside this volume causes a small fluctuation of particle as seen in the interval $[t_3, t_4]$ in Fig. 5.

Particle fluctuation in the z -direction

As can be seen from Fig. 5, after a number of time steps, the particle starts fluctuating in the z -direction at constant amplitude. This fluctuation is believed to be the effect of interior flow in a volume forming around the particle. Such volume doesn't exist at early time steps (t_1, t_2).

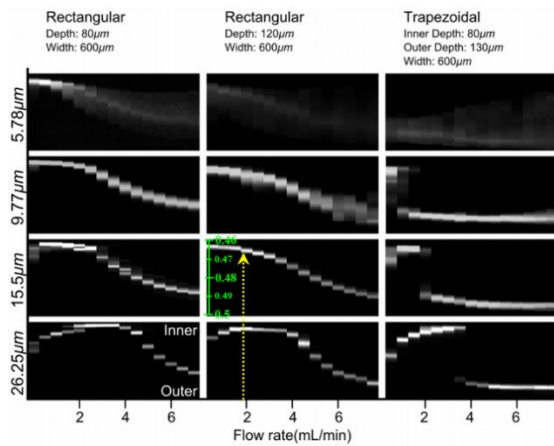


Fig. 6. Experimental results for particle position at channel outlet (Goufeng Guan *et al.* [6]). The case corresponding to our simulation model is marked by the yellow arrow ($120\mu\text{m}\times 600\mu\text{m}$, Rectangular cross section at $2\text{mL}/\text{min}$ flow rate). By comparing, we can see an agreement between the experiment result and the simulation result (Fig. 5).

4. Conclusion

In this study we presented an immersed boundary method for solving flow-structure interaction problem. The method uses a forcing term to enforce boundary condition for fluid flow on structure surface. The method was validated and applied to simulate the inertial focusing of solid particle in spiral channel, obtained result well matches with experimental observation. The method can be applied for predicting and optimizing design of microfluidics sorting and separating devices using in medicine.

Acknowledgments

This research is funded by the Hanoi University of Science and Technology under project number T2016-PC-026

References

- [1] D. Calhounm (2002). "A Cartesian grid method for solving the two-dimensional streamfunction vorticity equations in irregular regions". *J. Comput. Phys.*, 176:231–275.
- [2] M. Braza, P. Chassaing, and H. Ha Minh (1986). "Numerical study and physical analysis of the pressure and velocity fields in the near wake of a circular cylinder". *J. Fluid. Mech.*, 165:79–130.
- [3] C. Liu, X. Sheng, and C. H. Sung (1998). "Preconditioned multigrid methods for unsteady incompressible flows". *J. Comput. Phys.*, 139:35–57.
- [4] C. S. Peskin (2002). "The immersed boundary method". *Acta Numerica*, 11(2):479–517.
- [5] M. C. Lai and C. S. Peskin (2000). "An immersed boundary method with formal second order accuracy and reduced numerical viscosity". *J. Comput. Phys.*, 160:707–71
- [6] Guan, G. et al. (2013) "Spiral microchannel with rectangular and trapezoidal cross-sections for size based particle separation". *Sci. Rep.* 3, 1475